14.5 EFFECT OF THE LOWER BOUNDARY CONDITION ON TORNADO INTENSITY IN AN AXISYMMETRIC, CONSTANT-VISCOSITY, CLOSED MODEL OF TORNADOGENESIS

Robert Davies-Jones*
National Severe Storms Laboratory, NOAA
Norman, Oklahoma

1. INTRODUCTION

With a simple, axisymmetric, constant-viscosity model of tornadogenesis in a closed domain, Davies-Jones (2008; hereafter D-J) demonstrated how some tornadoes might form by Fujita's (1975) recycling mechanism. The model is without buoyancy forces because the atmosphere is neutrally stratified and there is neither evaporative cooling nor condensational warming. The initial condition (IC) consists of a Beltrami flow with a central updraft and mid-level mesocyclone, surrounded by an anticyclonic downdraft. The initial flow if left unperturbed decays slowly without changing pattern. Solid 'precipitation' particles are introduced above the updraft through the top boundary and fall at a constant speed in an annular rain curtain near the updraft/downdraft interface. In still air, the particles take 4 units of nondimensional time t (about 23 min) to reach the ground. The flow evolution is shown in D-J's Figs. 2-6. The associated precipitation-drag forces locally enhance the downdraft. The augmented downdraft and its outflow towards the axis transport air with moderately high angular momentum (AM) downward and inward, leading first to the development of a tornado cyclone on the ground, and then to formation of an intense tornado at the foot of the axis as the corner flow of the tornado cyclone collapses.

The model uses unrealistic "mixed" boundary conditions, namely no slip for the azimuthal (tangential) motion and no stress for the radial-vertical motion to accommodate the Beltrami flow as a solution of the numerical model (Shapiro 1993). Note however that Lewellen (1993 p. 24) did advocate using mixed conditions at the ground (no slip on v, the tangential wind, and free slip on u, the radial wind) in tornado models if a constant eddy viscosity is used because of the strong almost radial flow into the vortex in the lower part of the turbulent boundary layer of a tornado. Compared to a laminar boundary layer, a turbulent boundary layer has much sharper Compared to a laminar boundary layer, a turbulent boundary layer has much sharper gradients near the surface. Lewellen stated that a constant-viscosity model with a no-slip condition applied to u as well as v produces flow into the vortex that is weaker, deeper, more elevated and less radial than would occur in nature. At the other extreme, free-slip conditions on both u and v would eliminate the boundary layer and an end-wall vortex would not form.

Davies-Jones (2008) investigated the effect of the lower boundary condition (LBC) on the intensity of the tornado by performing simulations with three different LBCs, namely the mixed condition, free slip on both u and v, and no slip on both u and v. With a free-slip LBC a weak tornado cyclone develops at the surface even without rain. Davies-Jones (2008) used a modified IC that satisfied all three LBCs. Here the unmodified Beltrami IC is used because the flow instantly adapts to the boundary conditions, the results are basically the same, and the unmodified IC has certain advantages concerning physical interpretation of the results.

The mixed condition allows the strong, almost radially inward, flow next to the ground that occurs in vortices with turbulent boundary layers. An intense tornado develops in the form of a supercritical endwall vortex with an axial jet (Fiedler and Rotunno 1986). Measures of the near-surface intensification of this vortex relative to the tornado cyclone aloft, and the relative strengths of the maxima in the three wind components agree well with theoretical predictions (Fiedler and Rotunno 1986) and values for some numerically simulated turbulent vortices (Lewellen et al. 2000).

When the free-slip condition is used, the centrifugal force is unreduced near the ground, and, as the air spins up, is able in time to balance the inward pressure-gradient force. This balance occurs on the tornado-cyclone scale, not the mesocyclone scale, so a tornado cyclone still forms. Its central downdraft quickly reaches the ground, and produces a two-celled vortex structure with a widening inner cell. Its maximum tangential wind is 77% of the speed

*Corresponding author address: Dr. Robert Davies-Jones, NOAA/National Severe Storms Laboratory, National Weather Center, 120 David L. Boren Blvd., Norman, OK 73072-7323.
E-mail: Bob.Davies-Jones@noaa.gov

limit (Fiedler 1993, 1994), as corner flow collapse (CFC; Lewellen and Lewellen 2007) on the tornado-cyclone scale does not occur. The radial inflow and the maximum AM advection are much weaker in this case. The tornado cyclone does not have the frictional interaction with the ground that it needs to produce a strong tornado. It is significant however that a tornado cyclone forms even without interaction with the ground. In this model at least, the near-ground mesocyclone is just a passing phase during the collapse.

An end-wall vortex forms also with the no-slip LBC. However, it is considerably weaker than with the mixed LBC because of the reasons given by Lewellen (see above), and because the contours of AM do not descend as far. Consequently, the tornado develops slowly. It is stronger than the vortex in the free-slip case because the maximum inflow, which is now just above the ground, moves inward further and drives air with relatively high AM closer to the axis. In the simulations, the viscosity is low enough that this effect outweighs the loss of AM owing to the frictional torque (Rotunno 1979, Howells et al. 1988).

The purpose of this paper is to develop the conditions for CFC in more detail than in D-J.

2. CONDITIONS FOR CORNER FLOW COLLAPSE

At the surface, the ring of maximum inflow (which is a minimum of u) in the undisturbed Beltrami flow is stationary and slowly fills owing to viscous decay. When rain is introduced into the model and the mixed LBC is applied, this minimum of u moves inwards and deepens and corner flow collapse occurs. The following analysis establishes conditions for this process to occur. Since there is no surface inflow with the no-slip LBC, the method only applies to the mixed and free-slip LBCs. Comparison of these two cases is of considerable interest, however, because they produce the opposite extremes; the corner flow of the tornado cyclone collapses the most with the mixed LBC and does not collapse with the free-slip LBC.

Let $\rho(t)$ be the radius of maximum inflow as a function of time t. According to Petterssen's formulas (Petterssen 1956, pp. 48, 51), the minimum of u moves with the speed

$$c_\rho = -\left.\frac{\partial^2 u / \partial r \partial t}{\partial^2 u / \partial r^2}\right|_\rho \qquad (1)$$

and fills at the rate $\partial u/\partial t|_\rho$ where r is the radial coordinate and the subscript ρ denotes evaluation at the minimum. Along the ground (z = 0), the nondimensional radial equation of motion with Rayleigh friction is

$$\underset{T}{\frac{\partial u}{\partial t}} = \underset{A}{-u\frac{\partial u}{\partial r}} \underset{P}{-\frac{\partial \sigma}{\partial r}} \underset{C}{+\frac{M^2}{r^3}} \underset{F}{-\frac{1}{\mathrm{Re}}\lambda^2 u} \qquad (2)$$

where σ is the dry static energy (proportional to $p^{2/7}$ in the dry adiabatic atmosphere), p is pressure, $-\partial\sigma/\partial r$ is the radial pressure gradient force (RPGF), $M \equiv vr$ is angular momentum, and λ is a constant. The individual terms in (2) are: T, the tendency of u; A, the radial inertial force (excluding the centrifugal force); P the RPGF; C the centrifugal force; and F friction (either Rayleigh friction or viscous force). Note that an incompressible viscous Beltrami flow satisfies this equation because its viscous force reduces to Rayleigh friction. From (2), the minimum of u (where A = 0) fills at the rate

$$\left.\frac{\partial u}{\partial t}\right|_\rho = P_\rho + C_\rho + F_\rho \,. \qquad (3)$$

It deepens if $P + C + F$ is negative at its radius (Fig. 1). This requires the pressure-gradient force to be inward and the dominant force at $r = \rho$ ($P_\rho < 0$; $|P_\rho| > C_\rho + F_\rho$) because the centrifugal force is always outward and the Rayleigh friction force (and generally the viscous force as well) is also > 0 at the minimum since $u_\rho < 0$.

By differentiating (2) with respect to r, we obtain

$$\frac{\partial^2 u}{\partial r \partial t} = -u\frac{\partial^2 u}{\partial r^2} - \left(\frac{\partial u}{\partial r}\right)^2 - \frac{\partial^2 \sigma}{\partial r^2} + \frac{\partial}{\partial r}\left(\frac{M^2}{r^3}\right) - \frac{\lambda^2}{\mathrm{Re}}\frac{\partial u}{\partial r} \,. \qquad (4)$$

After substituting for the partial derivatives of u, the motion formula (1) becomes

$$\underset{\tau}{c_\rho} = \underset{\alpha}{u_\rho} \underset{\Pi}{-\left.\frac{\partial P / \partial r}{\partial^2 u / \partial r^2}\right|_\rho} \underset{\chi}{-\left.\frac{\partial C / \partial r}{\partial^2 u / \partial r^2}\right|_\rho} \underset{\Phi}{-\left.\frac{\partial F / \partial r}{\partial^2 u / \partial r^2}\right|_\rho} \qquad (5)$$

where $\partial^2 u/\partial r^2 > 0$ at the minimum and the terms are labeled in the second row. For the minimum to move inward, there has to a greater net inward force on the inner (axis) side of the minimum than on the outer side so that the differential of the net force is positive at $r = \rho$ (Fig. 1). The inertial force by itself moves the minimum radially inward at the advection speed u_ρ. The last three terms describe the propagation of the minimum. The friction term Φ has almost no influence on the motion of the minimum and can be omitted from (5) because

$\partial F/\partial r$ vanishes at the minimum for Rayleigh friction and is small there in the simulations.

First consider simulations that use the mixed condition so that $C = 0$ at the ground and

$$c_\rho = u_\rho - \left.\frac{\partial P / \partial r}{\partial^2 u / \partial r^2}\right|_\rho \qquad (6)$$

For the undisturbed Beltrami flow, $c_\rho = 0$ because $A + P = 0$. The u minimum slowly fills because $F_\rho > 0$. For the simulation with rain, the u minimum hardly moves and changes little from $t = 0$ to $t = 4$ (Fig. 2). It then moves steadily inwards and deepens until $t = 6$, the time that the tornado, which forms at $t = 5.4$, is at its peak intensity. From (6) the minimum moves inward slower than the advection speed if

$$\left.\partial P / \partial r\right|_\rho < 0 \text{ and } \left|\left.\partial P / \partial r\right|_\rho\right| < \left|\left.\partial I / \partial r\right|_\rho\right| \qquad (7)$$

The evolutions of the terms in (6) are shown in Fig. 3. The magnitudes of both α, the inward advection of the inflow maximum, and Π, the propagation owing to the differential of the pressure force at the inflow maximum, grow rapidly with time during the genesis and intensification of the tornado. However, the inward motion of the maximum inflow, τ, is relatively slow because α is nearly balanced by Π. This in consistent with (7). The motion owing to the differential friction term, Φ, is small, as claimed above

Deepening of the u minimum starts as precipitation reaches the ground (Fig. 4) owing to lower pressure on the inner side than on the outer side of the minimum [term P in (2)]. At the minimum the friction force F is outward and thus acts to fill the minimum. Because it is weaker than the pressure force there, the u minimum deepens. The inertial force A at the minimum should vanish at all times, but becomes nonzero during the tornado owing to numerical errors in the model's diagnostic computations when gradients become large.

More physical insight can be gained from a dynamical rather than kinematical approach. In (6), A and $A + P$ can be replaced by $-\partial k/\partial r$ and $-\partial B/\partial r$, respectively, where $k \equiv u^2/2$ is the kinetic-energy density (hereafter KE) at the surface and $B = \sigma + k$ is the surface Bernoulli function (sum of static and kinetic energies). Then (6) becomes

$$\frac{c_\rho}{u_\rho} = \left.\frac{-\partial^2 B / \partial r^2}{-\partial^2 k / \partial r^2}\right|_\rho, \qquad (8)$$

where $-\partial k^2/\partial r^2|_\rho$ is positive. Therefore, the minimum moves inwards if $\partial B^2/\partial r^2|_\rho < 0$. In the Beltrami flow, the Bernoulli function is zero everywhere with the KE exactly cancelled by negative static energy. In the rain simulation with the mixed LBC, the rain-induced downdraft descends to the surface and adds KE to the surface flow in its vicinity and also adds static energy through the stagnation-high effect. Consequently, the surface Bernoulli function B increases in this region. This is evident in Fig. 5, which is at a time ($t = 4.5$) when the mesocyclone is the only vortex present (the tornado cyclone forms at $t = 5$). The expanding downdraft has constricted the updraft, causing the mesocyclone to contract, spin up, and extend downward. The increased 'spin forcing' from above (Davies-Jones 2002) lowers the surface pressure near the axis. The KE is zero at the stagnation point (r, z) = (0, 0) so B is negative there. The surface static energy is lowest near the maximum inflow and mostly cancels the KE in this region. The radius of maximum inflow is moving inward because it is in a region where d^2B/dr^2 is negative. As previously discovered, the radius of maximum inflow moves inward at a speed that is slower than the advection speed because the inward pressure-gradient force is larger on the outer side ($r > \rho$) of the maximum inflow (Fig. 3), and the maximum inflow is intensifying because it is in a region where the radial pressure-gradient force is inward (Fig. 4).

When the LBC is free, the (never inward) centrifugal force enters into the equations for surface flow, which consist of (2) and the following equation for tangential flow:

$$\frac{\partial v}{\partial t} = -u\frac{\partial v}{\partial r} - \frac{uv}{r} + F_v \qquad (9)$$

where F_v is the azimuthal component of friction. In the simulation with the free LBC, the tangential winds in the tornado cyclone reach their maximum strength (0.77 times the speed limit) aloft at $t = 4.6$. To understand why a strong tornado does not develop in this case, we need to consider first the evolution of the v maximum. From (9) and Petterssen's formulas, we find that the v maximum intensifies at the rate

$$\left.\frac{\partial v}{\partial t}\right|_x = -\frac{u_x v_x}{r} + F_v \qquad (10)$$

and moves with the speed

$$c_x = u_x - \left.\frac{1}{-\partial^2 v / \partial r^2}\right|_x \left.\frac{\partial}{\partial r}\left(\frac{uv}{r}\right)\right|_x + \left.\frac{\partial F_v / \partial r}{-\partial^2 v / \partial r^2}\right|_x \qquad (11)$$

where $X(t)$ is the radius of maximum tangential velocity, F_v is the azimuthal component of friction, $v_x > 0$ and $-\partial^2 v/\partial r^2|_x > 0$. Thus, the azimuthal component of the centrifugal force, $-uv/r$, intensifies the maximum if $u_x < 0$ (as expected from conservation of AM) and azimuthal friction diminishes it provided that $F_v < 0$. If $u_x < 0$, the maximum moves inward slower than the its local advection speed if the sum of the azimuthal centrifugal and friction forces increase with increasing r at $r = X$. [In contrast to (5), model diagnostics show that the friction term cannot be omitted in the motion formula (11).] In the initial flow, at any given level except the top and ground where $v \equiv 0$, the maximum of v is collocated with the minimum of u. After one time step, there is very weak surface tangential wind with its maximum collocated with the u minimum owing to the LBC $\partial v/\partial z = 0$. At first, the v maximum is advected inward rapidly and intensifies owing to the near-conservation of AM. By $t = 2$ the radius of maximum surface tangential wind has contracted to tornado-cyclone scale (Fig. 6) and becomes almost stationary until t = 4.75 (Figs. 7 and 8) as its inward advection is balanced by outward propagation owing to the gradient of azimuthal friction at $r = X$ (Fig. 9). During this time the maximum tangential winds increase (Fig. 8) because air with higher angular momentum reaches the surface and is advected inwards. Azimuthal friction acts to decelerate the air, but is too small to prevent a net increase in tangential wind (Fig. 10). After $t = 5$, a central downdraft impacts the surface, and its outflow widens and weakens the vortex.

Now consider the evolution of the u minimum. It barely moves before $t = 3$ (Fig. 11) because the radial inertial force stays in balance with the RPGF (as in the IC), and the centrifugal force is weak at its location. In the simulation, the maximum of v remains on the axis side of the u minimum (Fig.11). Therefore, the differential of the radial centrifugal force is negative at the u minimum and acts in combination with the differential RPGF to reduce the inward speed of the minimum far below the advection speed (Fig. 12). The u minimum starts filling when the surface tangential wind at $r = \rho$ becomes super-cyclostrophic ($C_\rho + P_\rho > 0$; Fig. 13). Thus, when the LBC is free, the surface centrifugal force blocks catastrophic collapse of the corner flow and prevents a strong tornado.

3. CONCLUSIONS

In the D-J axisymmetric constant-viscosity model of tornadogenesis, the best of the three LBCs tested herein is no slip on the tangential motion and no stress on the radial flow. This LBC allows the strong almost radial flow that occurs in the lower part of the turbulent boundary layer of a strong vortex. An intense tornado with an axial jet forms by Fujita's recycling hypothesis. Measures of the near-surface intensification of the tornado relative to the tornado cyclone aloft, and the relative strengths of the maxima in the three wind components agree well with theoretical predictions and values for some numerically simulated vortices in turbulent flow.

When constant viscosity is used in conjunction with a no-slip condition ($u = v = 0$), the inflow is weaker, deeper, more elevated and less radial than occurs in a turbulent boundary layer of a vortex. An end-wall vortex still forms, but with significantly less intensification.

When a free-slip condition is used, a strong tornado does not form. The circle of maximum tangential wind contracts rapidly to the tornado-cyclone scale. This happens only with this LBC. Owing to a balance between the radial inertial and pressure forces, the radius of maximum inflow does not begin to decrease until the precipitation-induced downdraft impacts the surface. As the u minimum moves inward, it reaches a radius (outside the radius of maximum tangential wind) where the centrifugal force is large enough to prevent it from deepening further. Since the centrifugal force is larger on the axis side of the minimum than on the outer side, it prevents further progress of the minimum toward the axis. Thus, the centrifugal force at the surface does not allow the corner flow of the tornado cyclone to collapse in this case.

Acknowledgments. This work was supported in part by NSF grant ATM-0733539.

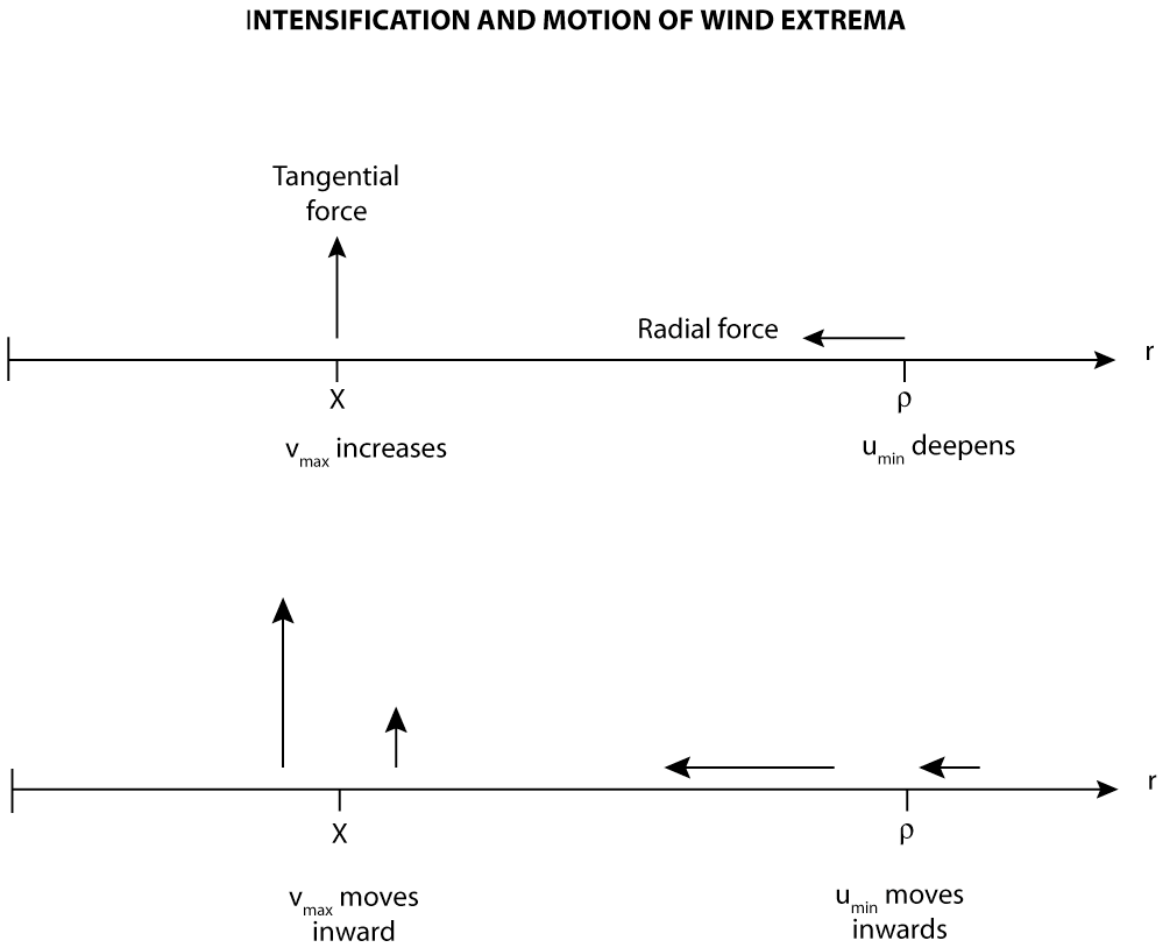

Fig. 1. Schematic showing how wind extrema intensify and move. The inflow maximum intensifies if the radial force at its radius ρ is inward, and it moves inward if there is a greater inward force on its inner side than on its outer side. The tangential-velocity maximum intensifies if the tangential force at its radius X is in the counterclockwise direction, and it moves inward if there is a larger tangential force in this direction on its inner side than on its outer side.

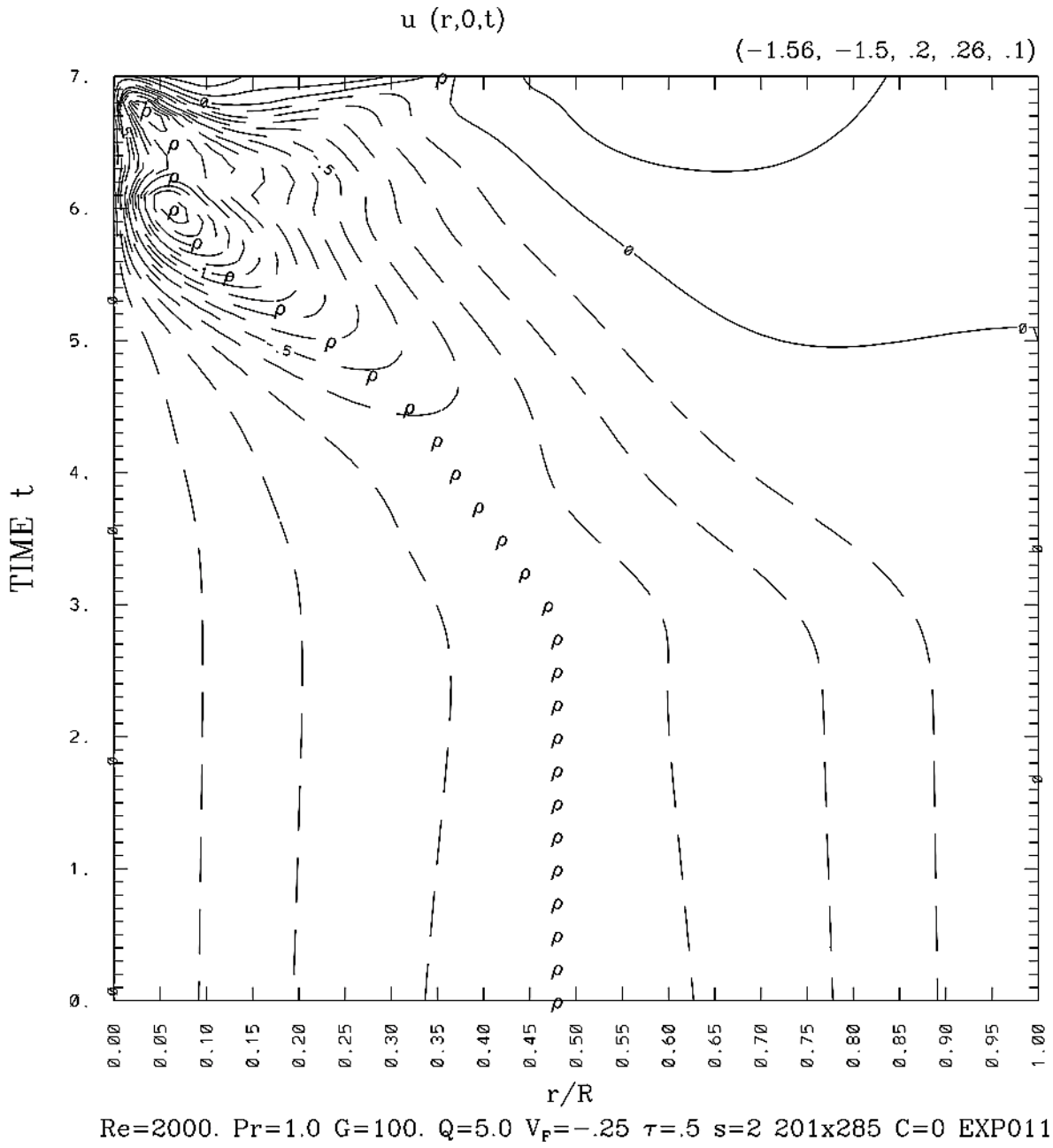

Fig. 2. The surface radial velocity as a function of nondimensional time and radius in the simulation that uses the mixed LBC. The letter ρ marks the position of the minimum radial velocity (maximum inflow) as a function of time.

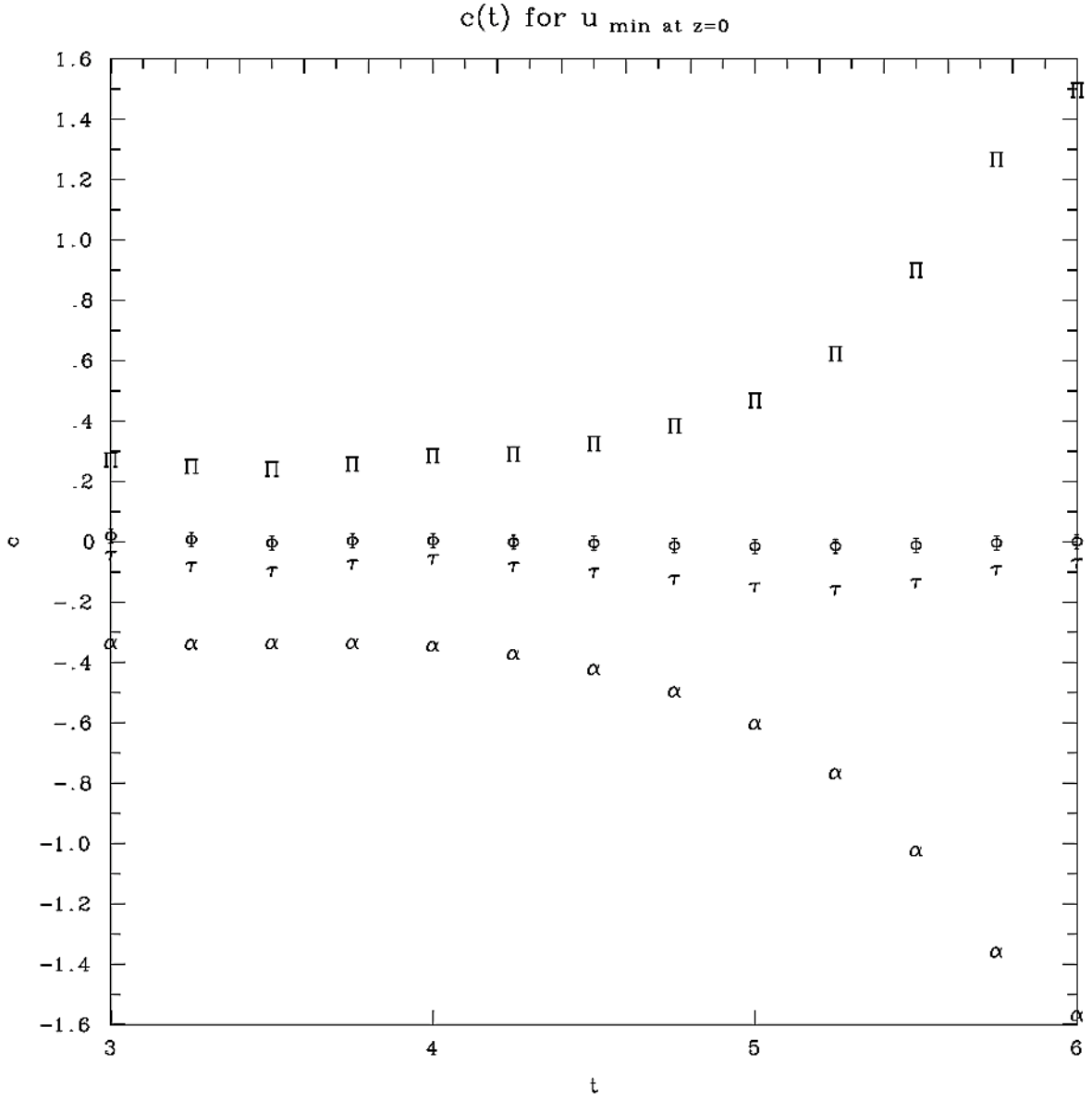

Fig. 3. The velocity $c(t)$ of the surface u minimum as determined by (5) in the simulation that uses the mixed LBC. The letters α, Π, Φ, τ indicate the advection velocity (owing to the radial inertial force), the propagation velocities owing to the radial pressure and friction forces, and the net motion.

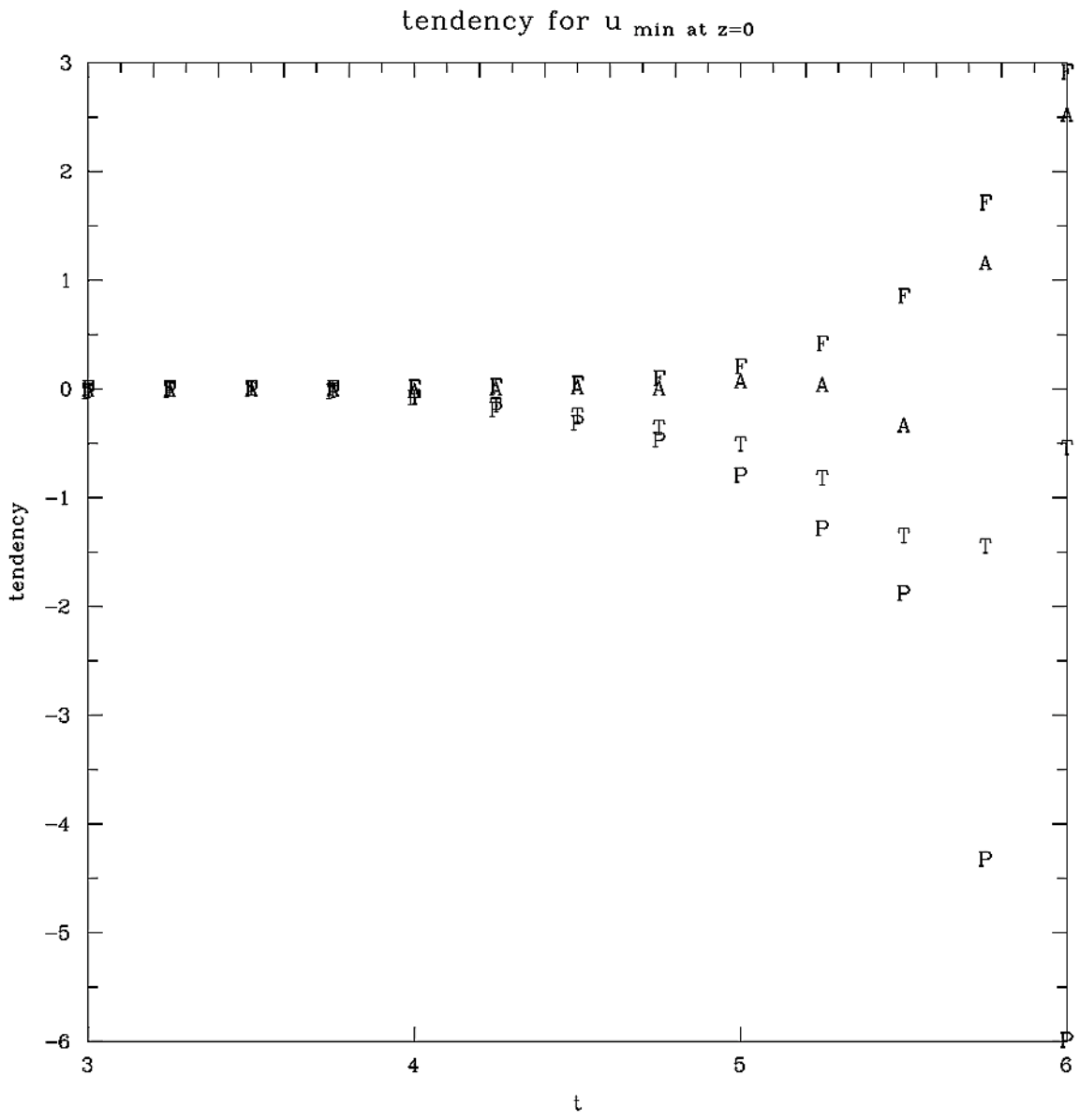

Fig. 4. The tendency $\partial u/\partial t|_\rho$ of the surface u minimum as determined by (3) in the simulation that uses the mixed LBC. The letters A, P, F, T indicate the contributions from the radial inertial, pressure, and friction forces, and the sum of all the radial forces. Note that the contribution from the inertial force should be zero.

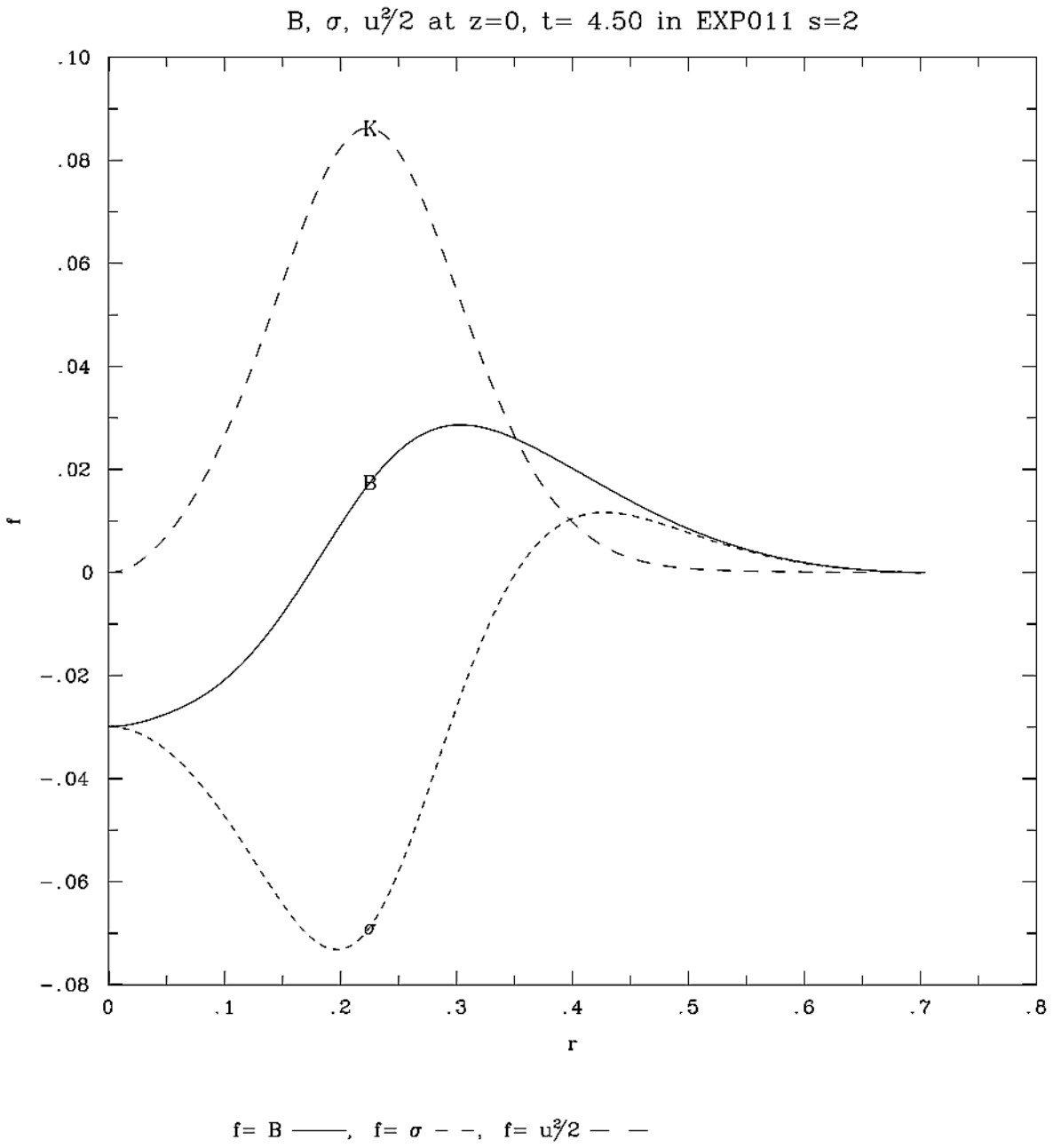

Fig. 5. The Bernoulli function, $B(r) = \sigma + u^2/2$ (solid), the static energy, $\sigma(r)$ (short dashes), and the specific kinetic energy, $k(r) = u^2/2$ (long dashes), at the surface at $t = 4.5$ in the simulation with the mixed LBC. The letters on the curve are at the radius of maximum surface inflow.

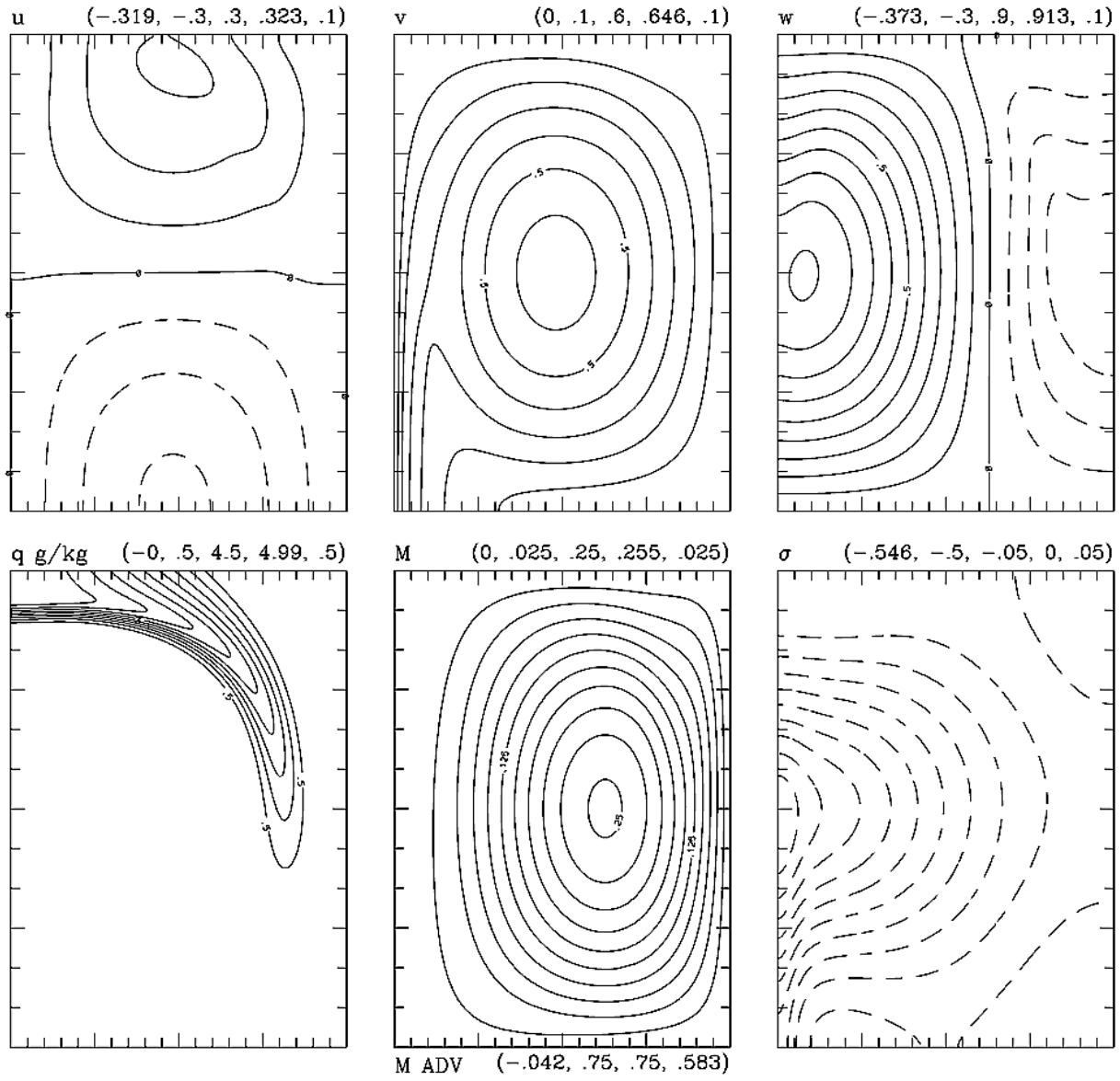

Fig. 6. Clockwise from top left: Fields at t = 2 of radial, tangential and vertical velocity (u, v, w), static energy σ, angular momentum M, and streamfunction ψ in the simulation with the free-slip LBC. The parentheses enclose the minimum value of the field, the minimum contour value, the maximum contour value, the maximum value of the field, and the contour interval, respectively, and generally every fifth contour is labeled. Negative contours are dashed. Tick marks are in increments of 0.05R (422.5 m) along the ground and H/12 (1 km) along the axis.

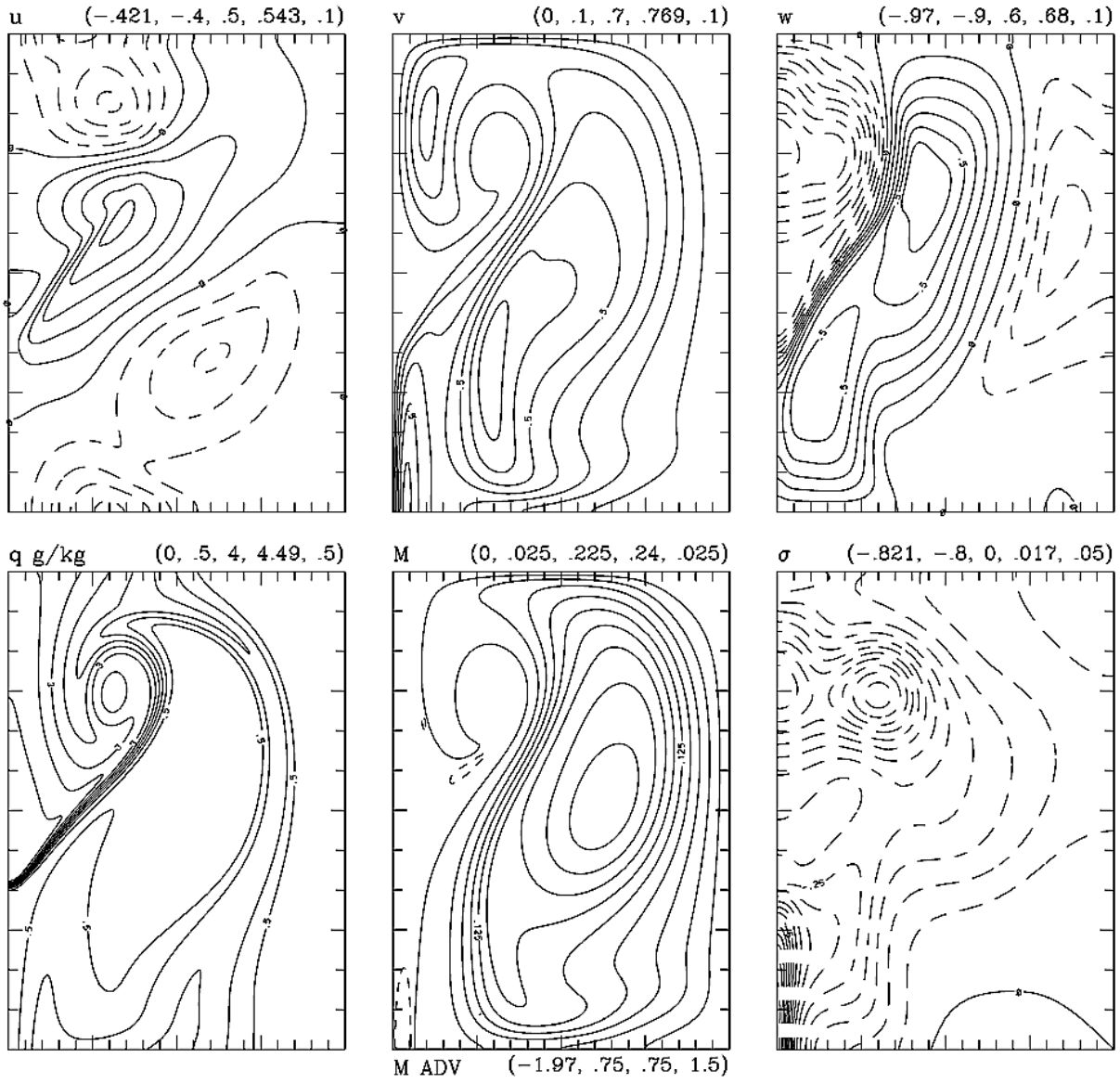

Fig. 7. As in Fig, 6 but at t = 4.75, and the .75 contour (dashed) of angular-momentum advection is included in the lower middle panel.

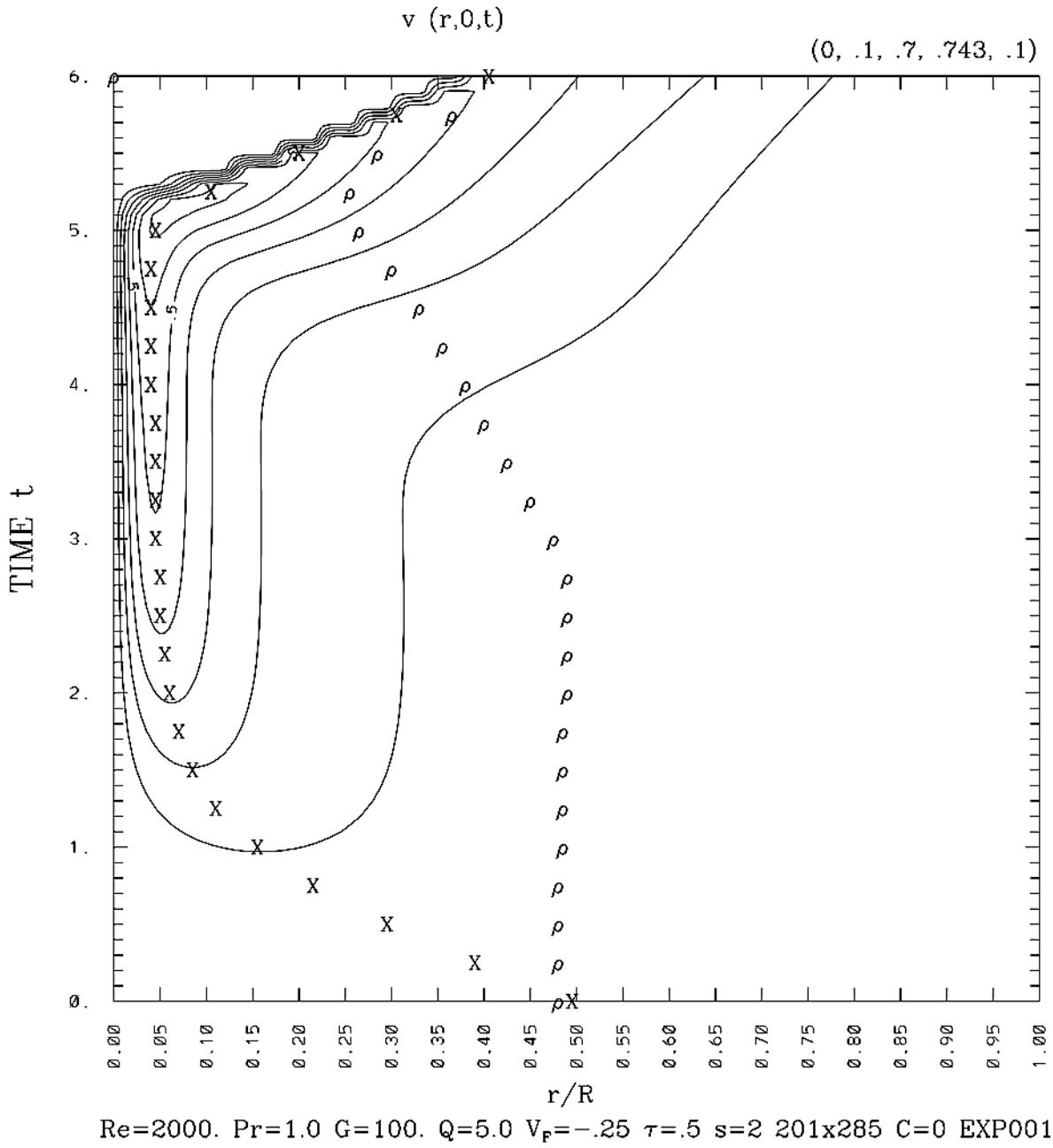

Fig. 8. The surface tangential velocity as a function of nondimensional time and radius in the simulation that uses the free-slip LBC. The letters X and ρ mark the positions of the maximum tangential velocity and the minimum radial velocity (maximum inflow), respectively, as a function of time.

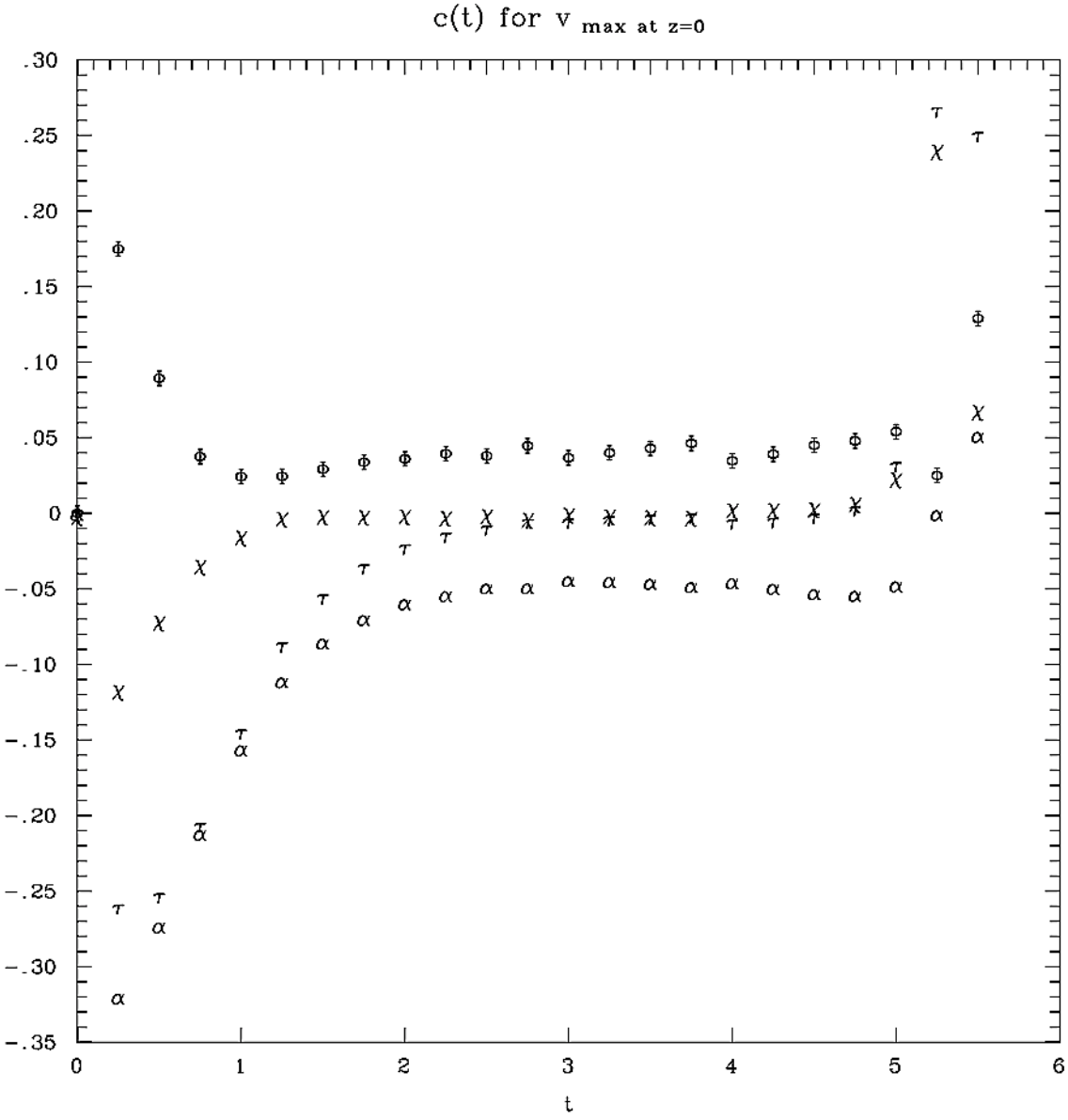

Fig. 9. The velocity $c(t)$ of the surface v maximum as determined by (11) in the simulation that uses the free-slip LBC. The letters α, Π, χ, Φ, τ indicate the advection velocity (owing to the tangential inertial force), the propagation velocities owing to the tangential centrifugal, pressure, and friction forces, and the net motion.

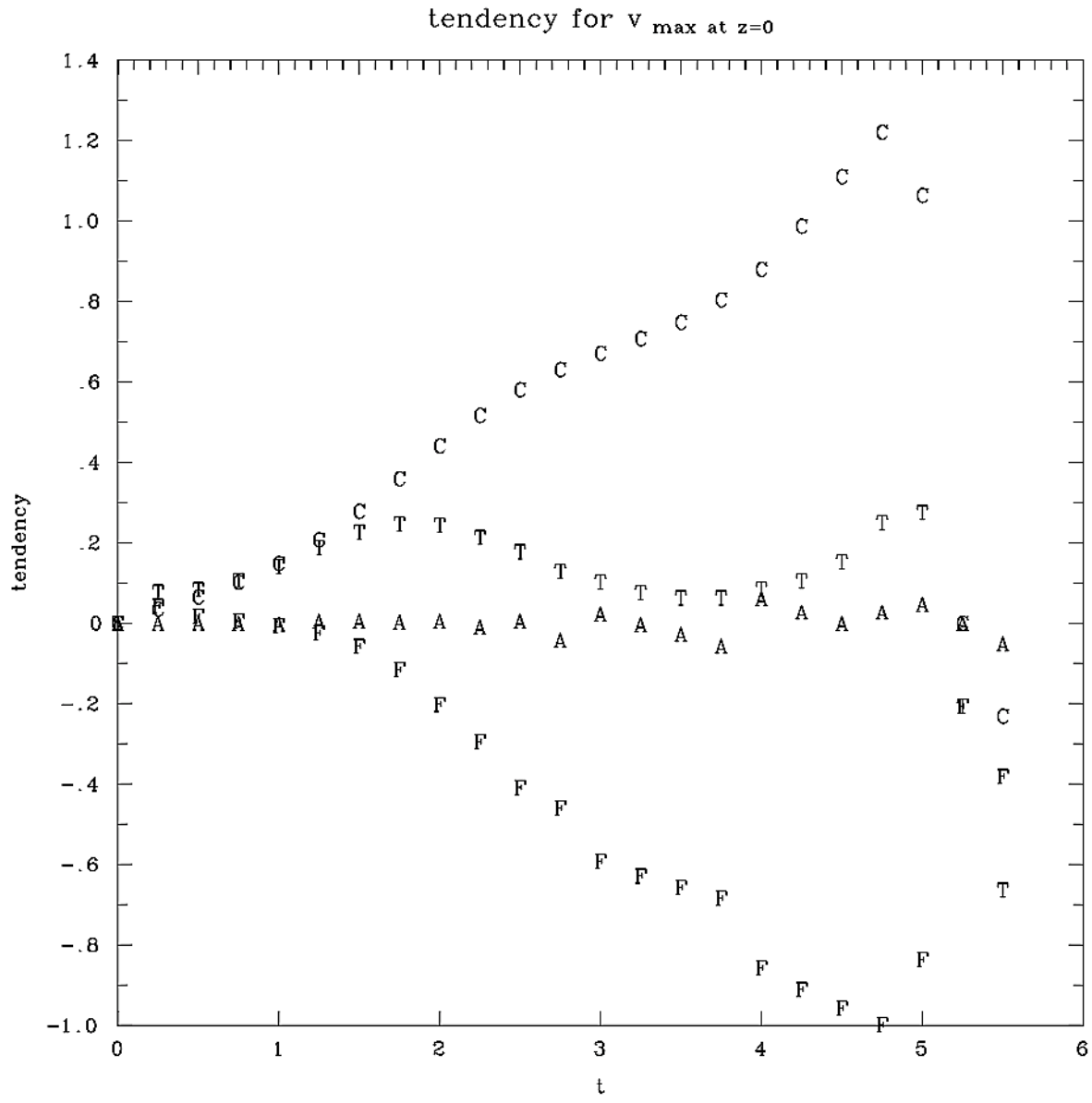

Fig. 10. The tendency $\partial v/\partial t|_\rho$ of the surface v maximum as determined by (10) in the simulation that uses the free-slip LBC. The letters A, C, P, F, T indicate the contributions from the tangential inertial, centrifugal, pressure, and friction forces, and the sum of all the tangential forces. Note that the contribution from the inertial force should be exactly zero.

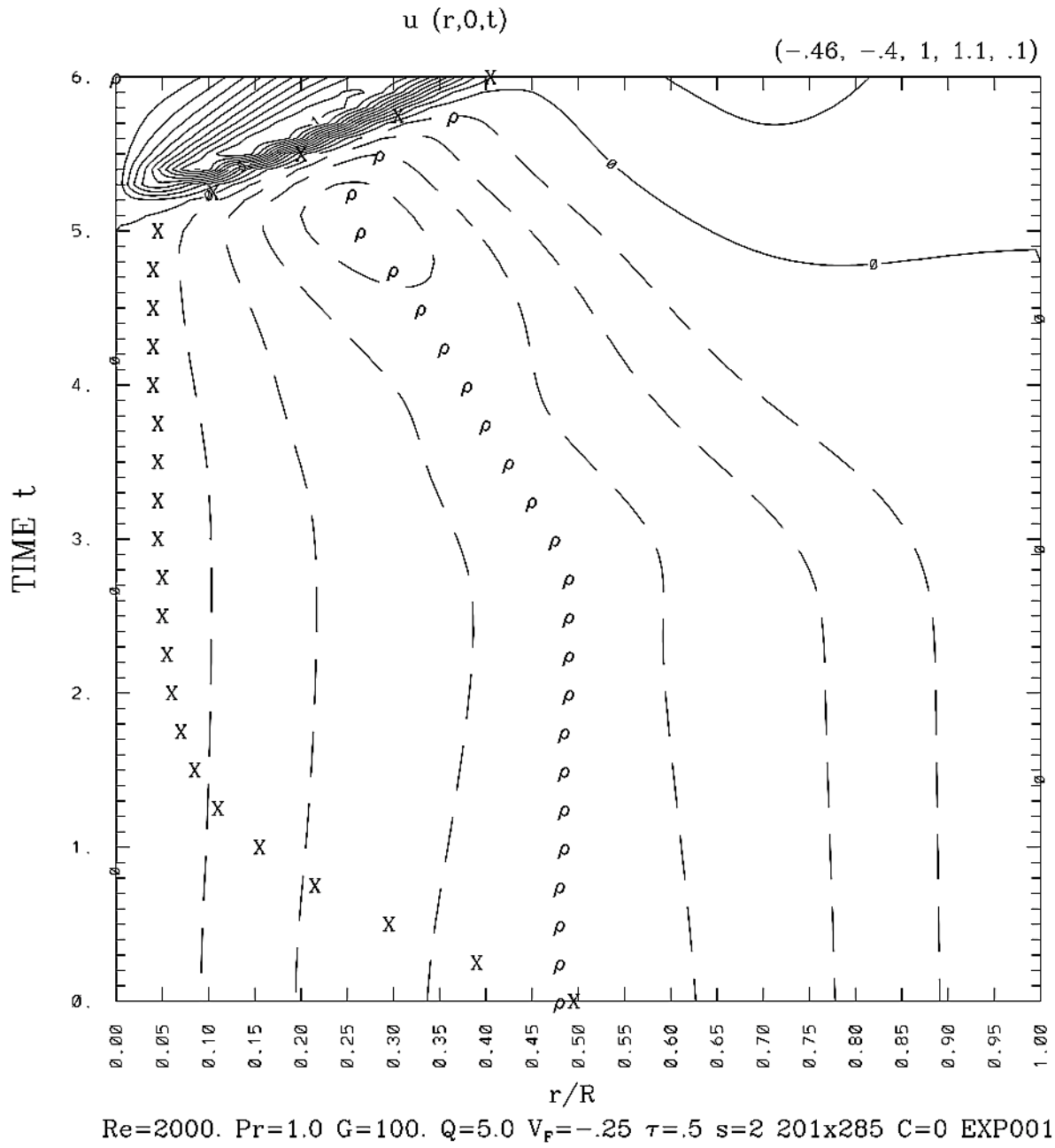

Fig. 11. The surface radial velocity as a function of nondimensional time and radius in the simulation that uses the free-slip LBC. The letters X and ρ mark the positions of the maximum tangential velocity and the minimum radial velocity (maximum inflow), respectively, as a function of time.

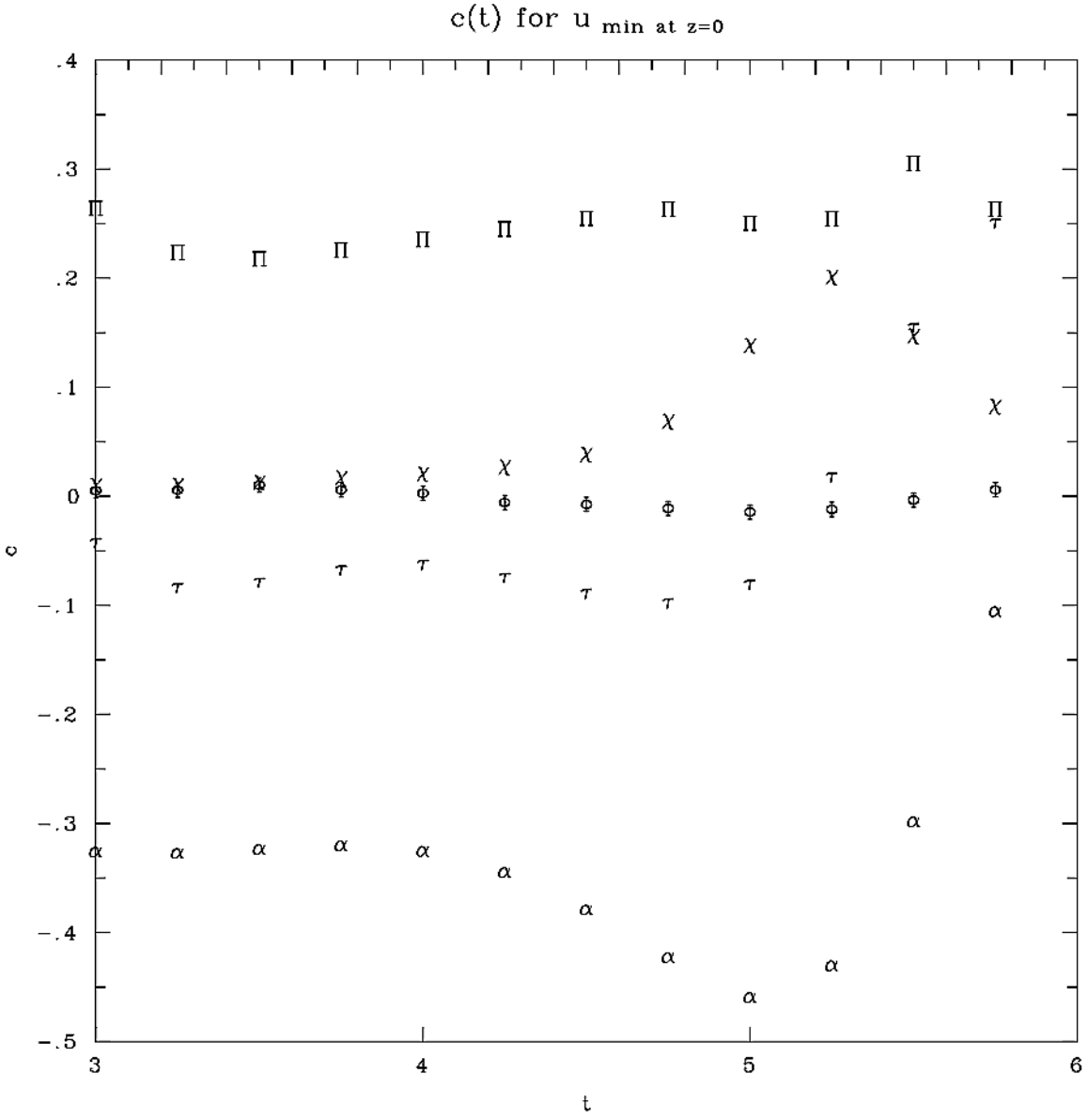

Fig. 12. The velocity $c(t)$ of the surface u minimum as determined by (5) in the simulation that uses the free-slip LBC. The letters α, χ, Π, Φ, τ indicate the advection velocity (owing to the radial inertial force), the propagation velocities owing to the radial pressure, centrifugal and friction forces, and the net motion.

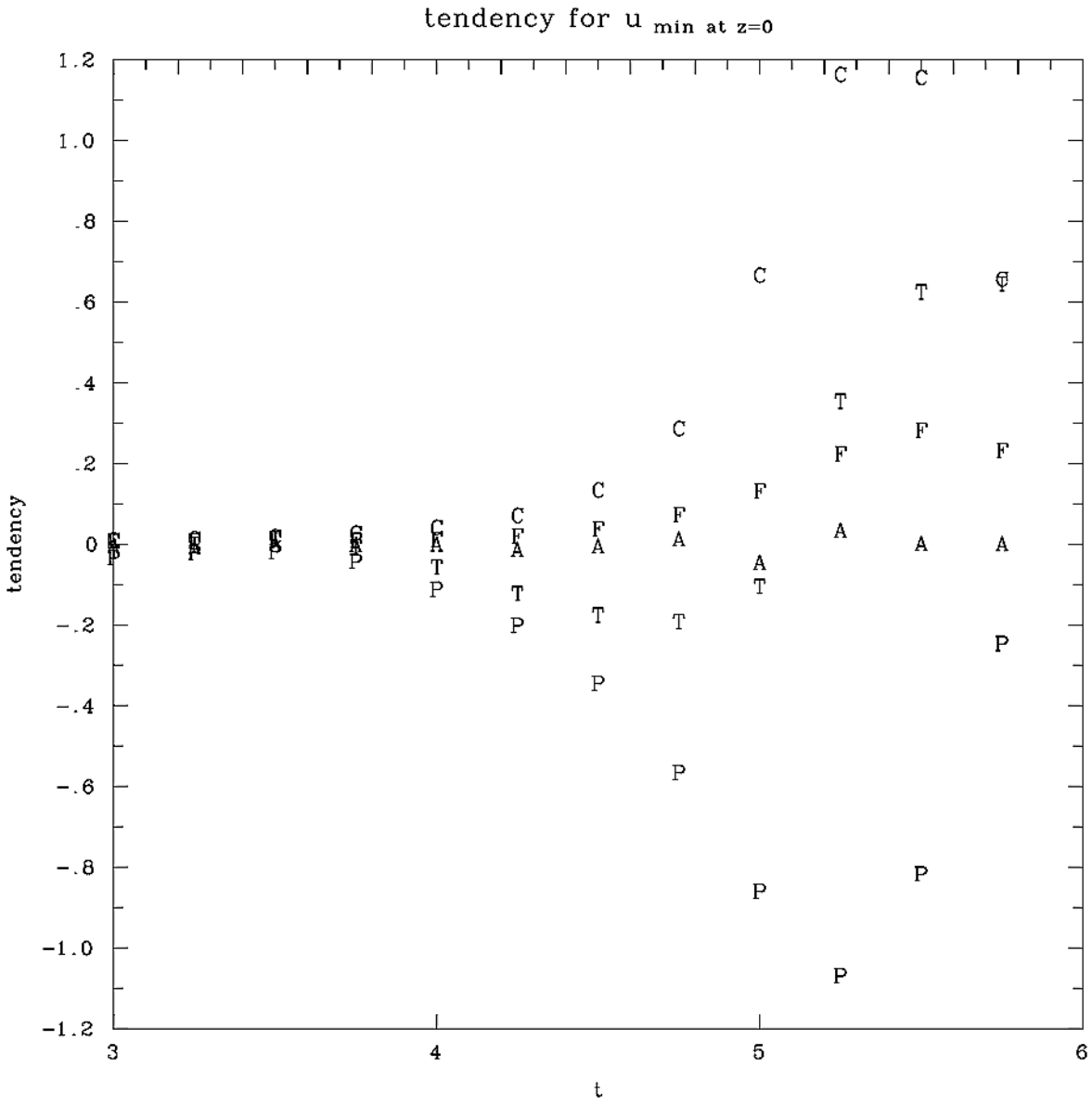

Fig. 13. The tendency $\partial u/\partial t|_\rho$ of the surface u minimum as determined by (3) in the simulation that uses the free-slip LBC. The letters A, C, P, F, T indicate the contributions from the radial inertial, centrifugal, pressure, and friction forces, and the sum of all the radial forces. Note that the contribution from the inertial force should be exactly zero.

4. REFERENCES

Davies-Jones, R., 2002: Linear and nonlinear propagation of supercell storms. *J. Atmos. Sci.,* **59,** 3178-3205.

Davies-Jones, R. P., 2008: Global properties of a simple axisymmetric simulation of tornadogenesis. Can a descending rain curtain in a supercell instigate tornadogenesis barotropically? *J. Atmos. Sci.,* **65,** 2469-2497.

Fiedler, B. H., 1993: Numerical simulation of axisymmetric tornadogenesis in forced convection. *The Tornado: Its Structure, Dynamics, Prediction and Hazards.* Geophys. Monogr., **79,** Amer. Geophys. Press, 41-48.

Fiedler, B. H., 1994: The thermodynamic speed limit and its violation in axisymmetric numerical simulations of tornado-like vortices. *Atmosphere-Ocean,* **32,** 335-359.

Fiedler, B. H., and R. Rotunno, 1986: A theory for the maximum windspeeds in tornado-like vortices. *J. Atmos. Sci.,* **43,** 2328-2340.

Fujita, T. T., 1975; New evidence from April 3-4, 1974 tornadoes. *Preprints*, 9th Conf. on Severe Local Storms, Norman, OK, Amer. Meteor. Soc., 248-255.

Howells, P. A. C., R. Rotunno, and R. K. Smith, 1988: A comparative study of atmospheric and laboratory-analogue numerical tornado-vortex models. *Quart. J. Roy. Meteor. Soc.*, **114**, 801-822.

Lewellen, W. S., 1993: Tornado vortex theory. *The Tornado: Its Structure, Dynamics, Prediction and Hazards.* Geophys. Monogr., **79,** Amer. Geophys. Press, 19-39.

Lewellen, D. C., and W. S. Lewellen, 2007: Near-surface vortex intensification through corner flow collapse. *J. Atmos. Sci.,* **64,** 2195-2209.

Lewellen, D. C., W. S. Lewellen, and J. Xia, 2000: The influence of a local swirl ratio on tornado intensification near the surface. *J. Atmos. Sci.,* **57,** 527-544.

Petterssen, S., 1956: *Weather Analysis and Forecasting. Volume I. Motion and Motion Systems.* 2nd ed., McGraw-Hill, 428 pp.

Rotunno, R., 1979: A study in tornado-like vortex dynamics. *J. Atmos. Sci.,* **36,** 140-155.

Shapiro, A., 1993: The use of an exact solution of the Navier-Stokes equations in a validation test of a three-dimensional nonhydrostatic numerical model. *Mon. Wea. Rev.,* **121,** 2420-2425.